Applied Physics Letters ARTICLE scitation.org/journal/apl

Modeling quantum light interference on a quantum computer

Cite as: Appl. Phys. Lett. **121**, 104001 (2022); doi: 10.1063/5.0103361
Submitted: 15 June 2022 · Accepted: 12 August 2022 ·
Published Online: 6 September 2022

Anton N. Vetlugin,[1,a)] Cesare Soci,[1,a)] and Nikolay I. Zheludev[1,2]

AFFILIATIONS

[1]Centre for Disruptive Photonic Technologies, SPMS, TPI, Nanyang Technological University, Singapore 637371
[2]Optoelectronics Research Centre and Centre for Photonic Metamaterials, University of Southampton, Southampton SO17 1BJ, United Kingdom

[a)]**Authors to whom correspondence should be addressed**: a.vetlugin@ntu.edu.sg and csoci@ntu.edu.sg

ABSTRACT

Modeling of photonic devices traditionally involves solving the equations of light–matter interaction and light propagation. Here, we demonstrate an alternative modeling methodology by reproducing the optical device functionality using a quantum computer. As an illustration, we simulate the quantum interference of light on a thin absorbing film. Such interference can lead to either perfect absorption or total transmission of light through the film, the phenomena attracting attention for data processing applications in classical and quantum information networks. We map the behavior of the photon in the interference experiment to the evolution of a quantum state of transmon, a superconducting charge qubit of the IBM quantum computer. Details of the real optical experiment are flawlessly reproduced on the quantum computer. We argue that the superiority of this methodology shall be apparent in modeling complex multi-photon optical phenomena and devices.

Quantum computing primarily aims to tackle computational problems such as integer factorization and unstructured search.[1] Beyond this, quantum computers provide a remarkable opportunity to simulate the behavior of quantum systems[2] with emphasis on quantum chemistry, quantum materials, particle physics, and cosmology.[3,4] Here, we are interested in the application of quantum computing to a simulation of phenomena of quantum photonics and devices based on the first principles, without relying on the fundamental equations. The core of the methodology is the creation of a model of a real optical experiment by developing a simulator-system correspondence, Fig. 1. To provide an illustrative example, we program the IBM quantum computer[5] to implement a model of the effect of a single-photon interference on a thin absorber.[6] This phenomenon[7,8] is of great interest for fundamental research[9–11] as well as for practical applications in light harvesting, detection,[12] sensing,[13] and photonics data processing.[14–16]

In classical optics, interference of coherent light waves on a thin absorber can eliminate the Joule losses of light energy or can lead to the total absorption of light depending on the phase relationship of the interfering waves.[7] Interference on a thin absorbing film was also extensively studied in quantum optics.[6,17–25] For instance, it was demonstrated that, despite the probabilistic nature of single-photon absorption in a traveling wave, the regimes of deterministic absorption and deterministic transmission of a photon can be achieved in a standing wave.[6] Below, we show how to model this experiment on a quantum computer.

A sketch of the setup, used in the experiment of Ref. 6, is shown in Fig. 2(a). The photon enters the interferometer through the 50:50 beam splitter (BS) (step 1) where it can be either transmitted to one or the other arms of the interferometer. The phase delay φ between the interferometer's arms is used to control the inner phase of a single photon wavefunction (step 2), so in the bra ket notation propagation through the interferometer can be written as

$$|A\rangle_P \rightarrow \frac{1}{\sqrt{2}}\left(|A\rangle_P + e^{i\varphi}|B\rangle_P\right), \tag{1}$$

where $|A\rangle_P$ and $|B\rangle_P$ identify the path of the photon, Fig. 2(a). This wavefunction interferes on a thin absorber (a plasmonic metamaterial film of a subwavelength thickness in the experiment) placed in the middle of the interferometer (step 3). The absorber is designed to have equal reflection and transmission coefficients of 25% and traveling wave absorption of 50%. The absorber becomes totally transparent if the photon is prepared in the anti-symmetric state, $\left(|A\rangle_P - |B\rangle_P\right)/\sqrt{2}$,

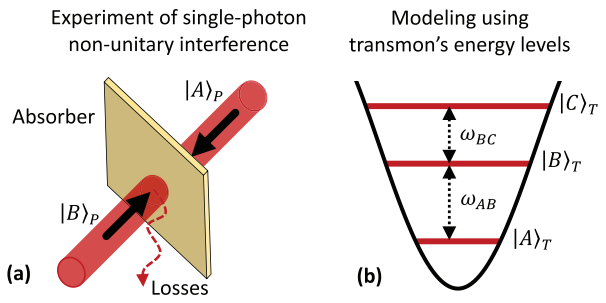

FIG. 1. Building a model of the photon interference experiment on a transmon. A correspondence is established between the optical interference experiment with a thin absorber (a) and a transmon of a quantum computer (b): The presence of a photon in the input ports $|A\rangle_P$ and $|B\rangle_P$ corresponds to states $|A\rangle_T$ and $|B\rangle_T$ of the trasmon. Losses are represented by the transition to the excited state $|C\rangle_T$.

$(\varphi = \pi)$. In contrast, the symmetric state of the photon, $(|A\rangle_P + |B\rangle_P)/\sqrt{2}$, $(\varphi = 0)$, is deterministically dissipated by the absorber. Indeed, the antisymmetric state corresponds to a standing wave in the interferometer with its node (zero electric field) coincident with the absorber's position:[25] the photon escapes dissipation due to the negligible electric field at the absorber. In contrast, the symmetric state corresponds to a standing wave with its anti-node (maximum electric field) at the absorber's position where light dissipation reaches 100%. For arbitrary φ, redistribution of the photon's wavefunction between the symmetric and anti-symmetric states defines the probability of the photon absorption and transmission as $\cos^2\frac{\varphi}{2}$ and $\sin^2\frac{\varphi}{2}$, correspondingly[17,25] (step 4). In the experiment, the probability of photon transmission is measured by sending a stream of photons through the interferometer and comparing the number of detected photons with and without the absorbing film, Fig. 2(a). By changing the phase of the interferometer φ, the transition between the regimes of "perfect absorption" and "perfect transmission" is observed, Fig. 4(a).

We have modeled this experiment on the IBM quantum computer with the ibmq_armonk[5] processor. The key functional element of the processor is a transmon[26] ("transmission-line shunted plasma oscillation qubit"), a type of superconducting charge qubit built around two Josephson junctions shunted with an additional capacitor. The transmon is an anharmonic quantum oscillator with a non-equidistance energy spectrum that allows the transition between two given states to be isolated and selectively addressed. We denote the ground, first excited, and second excited states of the transmon as $|A\rangle_T$, $|B\rangle_T$, and $|C\rangle_T$, respectively, where the frequency of transitions $|A\rangle_T \rightarrow |B\rangle_T$ and $|B\rangle_T \rightarrow |C\rangle_T$ are $\omega_{AB} \approx 4.97$ GHz and $\omega_{BC} \approx 4.62$ GHz, respectively.

Control of the transmons is performed by microwave signals from the coupled "drive" resonator.[27] For instance, in the oscillatory driving field at the resonant frequency ω_{AB}, the transmon will undergo the cyclic Rabi behavior, oscillating between the ground and first excited states. A microwave pulse transferring the transmon from the ground to the first excited state is known as a π-pulse, while a $\pi/2$-pulse leaves the transmon halfway through, in a superposition of the ground and first excited states. A sequence of such control pulses is used in the modeling to mimic different stages of the evolution of light

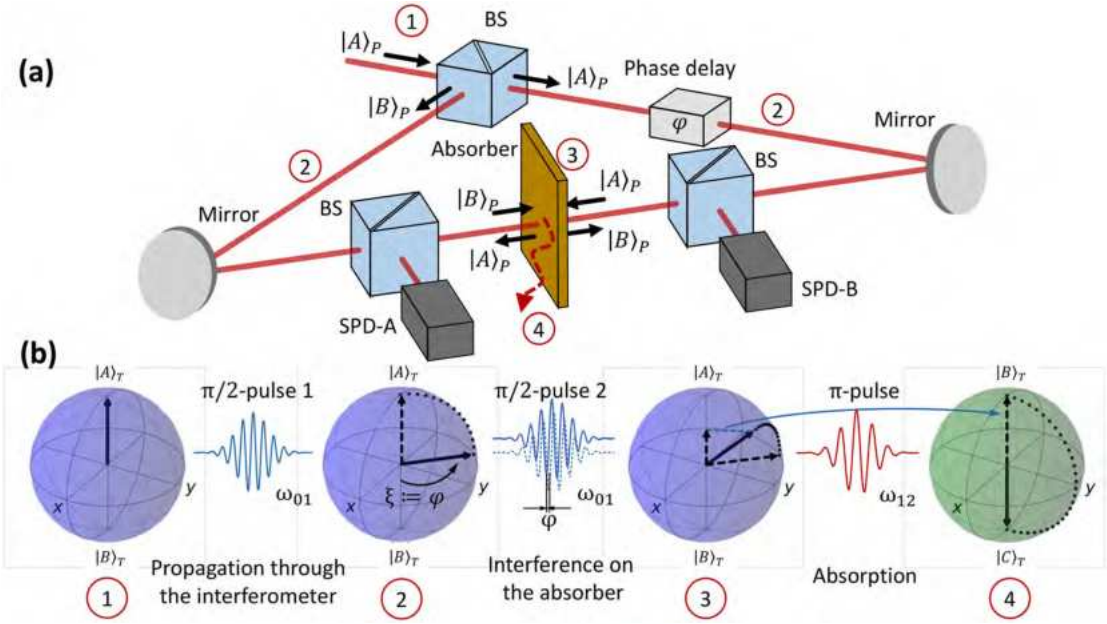

FIG. 2. Mapping evolution of a single photon in a lossy interferometer to the transmon's dynamics. (a) Photon enters the interferometer consisting of the input beam splitter (BS), phase delay, and mirrors. A thin absorber (plasmonic metamaterial) is placed in the middle of the interferometer. The outgoing light is detected by single photon detectors SPD-A and SPD-B. Steps of the photon's evolution are indicated by the numbers in circles. (b) The dynamics of the transmon is shown on the Bloch spheres representing its quantum state for different stages of the photon's evolution: ①→② A $\pi/2$-pulse at ω_{AB} changes the state of the transmon to mimic propagation of the photon through the interferometer. ②→③ The second $\pi/2$-pulse, also at ω_{AB}, but phase shifted on φ changes the state of the transmon to mimic interference on the absorber. ③→④ The action of a π-pulse at ω_{BC} mimics photon's absorption by moving the transmon to the higher excited state $|C\rangle_T$.

quantum in the interferometer. Here, it is important that the transmon's longitudinal and transverse relaxation times are of the order of a few tens of microseconds,[5] which is much longer than the experimental cycle that involves the consecutive application of three control microwave pulses of 0.6 μs each (see details below): natural relaxation of the transmon's excited states is insignificant during the experimental cycle. The energy state of the transmon is measured using a coupled "readout" microwave resonator: the amplitudes of quadratures of the probe signal reflected from the readout resonator identify the transmon's state using a state discriminator[28,29] calibrated prior to the experiment, Fig. 3.

Assuming other states are unpopulated, the state of the transmon in the basis of $|A\rangle_T$ and $|B\rangle_T$ is depicted as a vector on the Bloch sphere[1] [purple spheres in Fig. 2(b)] where the north and south poles of the sphere represent the states $|A\rangle_T$ and $|B\rangle_T$, respectively. Any transformation of the transmon state can be shown as a rotation(s) on the Bloch sphere. On the transmon, propagation through the interferometer and redistribution of the photon's wavefunction at the absorber is mimicked by driving the transmon with resonant microwave pulses at frequency ω_{AB}. Initiating the transmon in its ground state $|A\rangle_T$ corresponds to sending the photon through the input port of the interferometer (step 1 in Fig. 2). The transmon's state transformation, mimicking photon's propagation through the interferometer from step 1 to step 2, Eq. (1), is induced by a $\pi/2$-pulse at ω_{AB}. Redistribution of the photon's wavefunction between symmetric and anti-symmetric states in the middle of the interferometer (step 3) is replicated on the transmon by the second $\pi/2$-pulse at ω_{AB} with a phase shift φ compared to the first pulse. Here, the result of the modeling depends only on the phase difference between two consecutive $\pi/2$-pulses and not on their absolute phases. The second $\pi/2$-pulse rotates the anti-symmetric component of the wavefunction to the ground state and the symmetric component to the first excited state. To mimic absorption of the symmetric component of the photon's wavefunction (step 4), a π-pulse at ω_{BC} is applied, which brings the population of the first excited state of the transmon to the higher excided state $|C\rangle_T$. The π-pulse at ω_{BC} is off-resonant for the $|A\rangle_T \rightarrow |B\rangle_T$ transition and the population of the ground state, corresponding to photon's transmission through the absorber, is not affected. (The algorithm of quantum modeling is presented in the supplementary material and the corresponding Python code can be found in the data repository.)

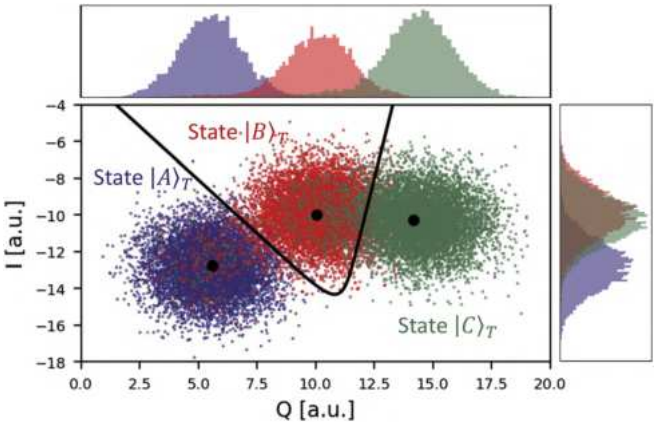

FIG. 3. Discrimination of transmon's states. To calibrate the readout channel, the transmon is initialized in one of its energy eigenstates multiple times (~8k for this experiment) followed by immediate measurement. Each measurement gives a point in the I–Q plane—purple for the prepared state $|A\rangle_T$, red—for the state $|B\rangle_T$, and green—for the state $|C\rangle_T$, where I and Q are two quadrature's of the readout signal. By applying linear discriminant analysis, the state discriminator is built (shown as a black solid line), and it is used to classify the transmon's state in latter experiments. Mean of each distribution is marked by a black point, and marginal plots show corresponding distributions for each quadrature.

In the optical experiment, a stream of single photons is sent through the interferometer with a fixed phase delay φ to find the probability of photon's transmission by measuring a large number of single-photon events, Fig. 4(a). To mimic this on the quantum computer, we run a number of trials (~1000) with a fixed phase difference φ between the first and second $\pi/2$-pulses. The probability of the transmon ending up in the ground "transmitted" state is presented in Fig. 4(b).

Figure 4(b) shows the results of quantum interference modeling for the absorber optimized to achieve a perfect absorption and for the absorber with parameters close to the real experiment. The modeling accurately reproduces the real experiment exhibiting the regimes of perfect absorption and perfect transmission depending on the phase φ. Nearly perfect visibility of the simulated dependence of absorption probability on φ is achieved with the optimized absorber (50% traveling wave absorption). In the experiment of Ref. 6, the metamaterial's absorption was 45%, i.e., off the optimized value. That explains the lower visibility observed in the real experiment that shows some residual absorption for $\varphi = \pm\pi$ and non-zero transmission for $\varphi = 0$ due to unperfect interference cancelation on the absorber, Fig. 4(a). To model the non-optimized absorber, the amplitude of the second pulse controlling transmon was decreased by about 30% from the amplitude of the $\pi/2$-pulses. Such adjustment of the control pulse leads to the absorption increase in the anti-symmetric component and corresponding absorption decrease in the symmetric component of the transmon's wavefunction mimicking interference disbalance in the real experiment.

Experiments on quantum non-unitary interference[6,18–20,22–24,30] have been addressing the regime of "symmetric" illumination of an absorber when a photon is present on both sides of the absorber with equal probabilities. Modeling of this scenario is implemented here via accessing the states on the equator of a Bloch sphere, inset in Fig. 4(b). To study interference beyond this regime, a substantial modification of the setup is required replacing a fixed 50:50 (transmission to reflection ratio, T:R) beam splitter at the input of the interferometer with a variable beam splitter (in the form of the additional interferometer[31]). In contrast, modeling the regimes of "asymmetric" illumination using a transmon is straightforward. In Figs. 4(c) and 4(d), the results of such modeling are shown. The only difference from the above-described procedure is the changed amplitude of the first pulse, which now induces $\pi/3$- or $\pi/8$-rotation, respectively, simulating splitting ratios of input beam splitter 25:75 or 4:96.

Modeling optical phenomena on a quantum computer can be developed further in different ways. By incorporating higher excited states, one can consider various models of losses and non-unitary transformation, incorporate the mechanisms of radiative, and non-radiative decay. At the same time, employment of higher excited states would allow studying the propagation of a single photon through a large-scale optical networks[32–37] and quantum memories.[30,38] For instance, any passive optical network can be represented as a sequence of phase

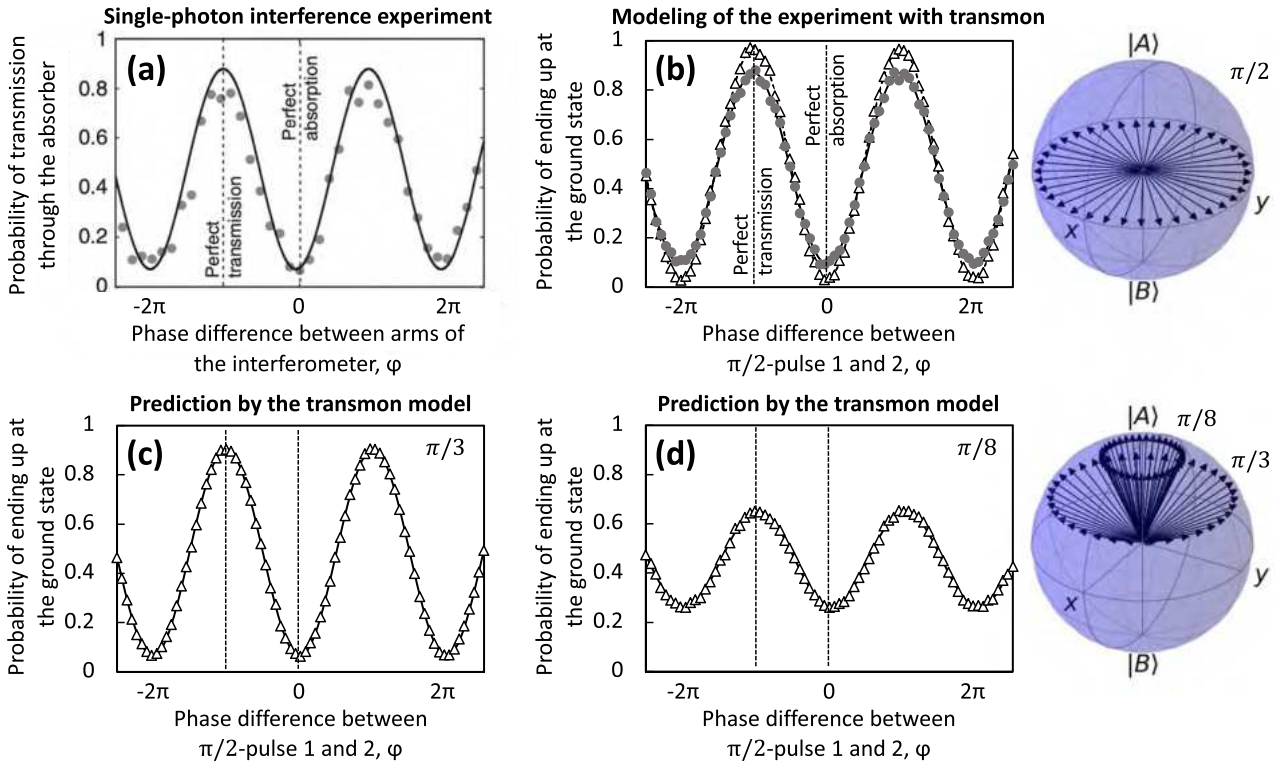

FIG. 4. Simulation of the quantum interference experiment with a quantum computer. (a) The probability of a single photon transmission through the absorber is a function of φ, the phase difference between the arms of interferometer. Note the regimes of perfect absorption ($\varphi = 0$) and perfect transmission ($\varphi = \pm\pi$). (b) The probability of photon's transmission is represented by the probability of finding the transmon in the ground state: modeling for the optimized absorber (empty triangles and dashed fitting line) and absorber with parameters close to the experiment (gray circles and solid fitting line). This probability depends on the phase delay φ between the first and second $\pi/2$-pulses acting on the transmon. This phase delay represents the optical pass phase difference between the arms of interferometer. (c) and (d) Using the transmon model to predict the asymmetric regimes of single-photon interference not demonstrated experimentally. Insets on the right show corresponding sets of transmon's states prepared by the first microwave pulse; the polar angle is indicated for each set of states. Panel (a) is reproduced with permission from Roger *et al.*, Nat. Commun. **6**, 7031 (2015).[6] Copyright 2015 Authors, licensed under a Creative Commons Attribution (CC BY).

shifting operations applied to a single mode (waveguide and fiber), beam splitting operations applied between two modes, and, for non-unitary networks, lossy components.[32,34,35,39] In the modeling experiment, each optical mode, as well as lossy channels, should be mapped to one of the transmon eigenstates. An optical beam splitter can be modeled by applying the resonant pulse between two corresponding eigenstates where the splitting ratio is controlled by the microwave pulse amplitude, and optical phase shifts are controlled, for instance, by the phase shifts between the microwave pulses applied to the transmon. Optical lossy components can be modeled in a fashion employed in this paper. Practical limitations on the size of the modeled optical network will be defined mainly by the transmon relaxation times.

By exploiting multiple transmons, the dynamics of other quantum states of light,[25] such as NOON[18] and entangled[23] and more complex states, can be studied. For instance, one can easily generate and study the evolution of complex quantum states using cloud quantum computing while generating such states on the optical table is a challenging task.

Beyond quantum light interference, other optical devices[40] and phenomena can be modeled by building a simulator-system correspondence. For instance, using the mathematical identity of the Bloch and Poincare sphere, a model of experiments involving multidimensional structured quantum light[41,42] can be developed.

In conclusion, the methodology of building a model of an optical experiment on a quantum computer provides a universal platform for studying and analysis of quantum optics phenomena and systems. We argue that modeling on a quantum computer with a discrete spectrum of transmon is the next, quantum step of developing analog computing in photonics since the wide-spread use of classical analog computers to solve problems of non-linear optics in the 1970s.[43]

See the supplementary material for additional details on the implementation of quantum modeling.

The authors are grateful to IBM for free access to services provided by the IBM Quantum Researchers Program. The views expressed are those of the authors and do not reflect the official policy or position of IBM or the IBM Quantum team. This work was supported by the Singapore Ministry of Education [No. MOE2016-T3-1-006 (S)], the Quantum Engineering Programme of

the Singapore National Research Foundation (Nos. NRF-QEP1 and NRF-QEP2-01-P01), and the UK's Engineering and Physical Sciences Research Council (Grant No. EP/M009122/1).

AUTHOR DECLARATIONS

Conflict of Interest

The authors have no conflicts to disclose.

Author Contributions

A.N.V conceived the idea and performed the modeling experiment; A.N.V. and N.I.Z. wrote the manuscript; all co-authors discussed the results. N.I.Z. & and C.S. co-supervised the project.

Anton N. Vetlugin: Conceptualization (equal); Data curation (equal); Methodology (equal); Software (equal); Visualization (equal); Writing – original draft (equal); Writing – review & editing (equal). **Cesare Soci:** Data curation (equal); Funding acquisition (equal); Methodology (equal); Project administration (equal); Supervision (equal); Writing – review & editing (equal). **Nikolay I. Zheludev:** Conceptualization (equal); Data curation (equal); Funding acquisition (lead); Methodology (equal); Project administration (lead); Supervision (equal); Writing – review & editing (equal).

DATA AVAILABILITY

The data that support the findings of this study are openly available in NTU research data repository DR-NTU (data) at https://doi.org/10.21979/N9/4B0V0S.

REFERENCES

[1]M. A. Nielsen and I. L. Chuang, *Quantum Computation and Quantum Information: 10th Anniversary Edition* (Cambridge University Press, 2010).
[2]R. P. Feynman, "Simulating physics with computers," Int. J. Theor. Phys. **21**, 467–488 (1982).
[3]E. Altman, K. R. Brown, G. Carleo *et al.*, "Quantum simulators: Architectures and opportunities," PRX Quantum **2**, 017003 (2021).
[4]C. Noh and D. G. Angelakis, "Quantum simulations and many-body physics with light," Rep. Prog. Phys. **80**, 016401 (2017).
[5]See https://quantum-computing.ibm.com/ for "IBM Quantum" (2021).
[6]T. Roger, S. Vezzoli, E. Bolduc *et al.*, "Coherent perfect absorption in deeply subwavelength films in the single-photon regime," Nat. Commun. **6**, 7031 (2015).
[7]J. F. Zhang, K. F. MacDonald, and N. I. Zheludev, "Controlling light-with-light without nonlinearity," Light Sci. Appl. **1**, e18 (2012).
[8]Y. D. Chong, L. Ge, H. Cao *et al.*, "Coherent perfect absorbers: Time-reversed lasers," Phys. Rev. Lett. **105**, 053901 (2010).
[9]W. Wan, Y. D. Chong, L. Ge *et al.*, "Time-reversed lasing and interferometric control of absorption," Science **331**, 889–892 (2011).
[10]D. G. Baranov, A. Krasnok, and A. Alù, "Coherent virtual absorption based on complex zero excitation for ideal light capturing," Optica **4**, 1457–1461 (2017).
[11]A. Müllers, B. Santra, C. Baals *et al.*, "Coherent perfect absorption of nonlinear matter waves," Sci. Adv. **4**, eaat6539 (2018).
[12]M. K. Akhlaghi, E. Schelew, and J. F. Young, "Waveguide integrated superconducting single-photon detectors implemented as near-perfect absorbers of coherent radiation," Nat. Commun. **6**, 8233 (2015).
[13]E. Plum, K. F. MacDonald, X. Fang *et al.*, "Controlling the optical response of 2D matter in standing waves," ACS Photonics **4**, 3000–3011 (2017).
[14]X. Fang, K. F. MacDonald, and N. I. Zheludev, "Controlling light with light using coherent metadevices: All-optical transistor, summator and invertor," Light Sci. Appl. **4**, e292 (2015).
[15]A. Xomalis, I. Demirtzioglou, E. Plum *et al.*, "Fibre-optic metadevice for all-optical signal modulation based on coherent absorption," Nat. Commun. **9**, 182 (2018).
[16]M. Papaioannou, E. Plum, and N. I. Zheludev, "All-optical pattern recognition and image processing on a metamaterial beam splitter," ACS Photonics **4**, 217–222 (2017).
[17]S. M. Barnett, J. Jeffers, A. Gatti *et al.*, "Quantum optics of lossy beam splitters," Phys. Rev. A **57**, 2134–2145 (1998).
[18]T. Roger, S. Restuccia, A. Lyons *et al.*, "Coherent absorption of N00N states," Phys. Rev. Lett. **117**, 023601 (2016).
[19]C. Altuzarra, S. Vezzoli, J. Valente *et al.*, "Coherent perfect absorption in metamaterials with entangled photons," ACS Photonics **4**, 2124–2128 (2017).
[20]B. Vest, M. C. Dheur, E. Devaux *et al.*, "Anti-coalescence of bosons on a lossy beam splitter," Science **356**, 1373–1376 (2017).
[21]A. Lyons, D. Oren, T. Roger *et al.*, "Coherent metamaterial absorption of two-photon states with 40% efficiency," Phys. Rev. A **99**, 011801 (2019).
[22]A. N. Vetlugin, R. Guo, A. Xomalis *et al.*, "Coherent perfect absorption of single photons in a fiber network," Appl. Phys. Lett. **115**, 191101 (2019).
[23]A. N. Vetlugin, R. Guo, C. Soci *et al.*, "Anti-Hong-Ou-Mandel effect with entangled photons," arXiv:2105.05444 (2021).
[24]S. Yanikgonul, R. Guo, A. Xomalis *et al.*, "Phase stabilization of a coherent fiber network by single-photon counting," Opt. Lett. **45**, 2740–2743 (2020).
[25]A. N. Vetlugin, "Coherent perfect absorption of quantum light," Phys. Rev. A **104**, 013716 (2021).
[26]J. Koch, T. M. Yu, J. Gambetta *et al.*, "Charge-insensitive qubit design derived from the Cooper pair box," Phys. Rev. A **76**, 042319 (2007).
[27]P. Krantz, M. Kjaergaard, F. Yan *et al.*, "A quantum engineer's guide to superconducting qubits," Appl. Phys. Rev. **6**, 021318 (2019).
[28]See https://qiskit.org/textbook/preface.html (Chapter 6) for information on calibration of the transmon of the IBM quantum computers.
[29]T. Alexander, N. Kanazawa, D. J. Egger *et al.*, "Qiskit pulse: Programming quantum computers through the cloud with pulses," Quantum Sci. Technol. **5**, 044006 (2020).
[30]A. N. Vetlugin, R. Guo, C. Soci *et al.*, "Deterministic generation of entanglement in quantum networks by coherent absorption of a single photon," Phys. Rev. A **106**, 012402 (2022).
[31]D. A. B. Miller, "Perfect optics with imperfect components," Optica **2**, 747–750 (2015).
[32]M. Reck, A. Zeilinger, H. J. Bernstein *et al.*, "Experimental realization of any discrete unitary operator," Phys. Rev. Lett. **73**, 58–61 (1994).
[33]D. A. B. Miller, "Self-configuring universal linear optical component," Photonics Res. **1**, 1–15 (2013).
[34]W. R. Clements, P. C. Humphreys, B. J. Metcalf *et al.*, "Optimal design for universal multiport interferometers," Optica **3**, 1460–1465 (2016).
[35]N. Tischler, C. Rockstuhl, and K. Słowik, "Quantum optical realization of arbitrary linear transformations allowing for loss and gain," Phys. Rev. X **8**, 021017 (2018).
[36]K. Tschernig, R. de J. León-Montiel, A. Pérez-Leija *et al.*, "Multiphoton synthetic lattices in multiport waveguide arrays: Synthetic atoms and Fock graphs," Photonics Res. **8**, 1161–1170 (2020).
[37]O. Hernández and I. Liberal, "Generalized approach to quantum interference in lossy N-port devices via a singular value decomposition," Opt. Express **30**, 31267–31286 (2022).
[38]A. N. Vetlugin and I. V. Sokolov, "Multivariate quantum memory as controllable delayed multi-port beamsplitter," Europhys. Lett. **113**, 64005 (2016).
[39]O. Hernández, A. Ortega-Gomez, M. Bravo *et al.*, "Quantum interference in Wilkinson power dividers," Laser Photonics Rev. **16**, 2200095 (2022).
[40]E. A. Chan, G. Adamo, S. A. Aljunid *et al.*, "Plasmono-atomic interactions on a fiber tip," Appl. Phys. Lett. **116**, 183101 (2020).
[41]Y. Shen, Z. Wang, X. Fu *et al.*, "SU(2) Poincaré sphere: A generalized representation for multidimensional structured light," Phys. Rev. A **102**, 031501 (2020).
[42]Z. Wang, R. Long, Z. Wan *et al.*, "Transverse traveling-wave and standing-wave ray-wave geometric beams," Front. Photonics **3**, 855214 (2022).
[43]D. R. Solli and B. Jalali, "Analog optical computing," Nat. Photonics **9**, 704–706 (2015).